International Journal of Heat and Technology
Vol. 43, No. 2, April, 2025, pp. 415-427
Journal homepage: http://iieta.org/journals/ijht

Numerical Investigation of Erosion Mechanisms in L-Shaped Pipeline Bends with Solid Impurities Using CFD

Abhishek Agarwal[1*], Hasddin[2], Okta Bani[3], Masengo Ilunga[4]

[1] Department of Mechanical Engineering, College of Science & Technology, Royal University of Bhutan, Phuentsholing 21101, Bhutan
[2] Department of Urban and Regional Planning, Faculty of Engineering, Lakidende University, Unaaha 93461, Indonesia
[3] Department of Chemical Engineering, Universitas Sumatera Utara, Medan 20123, Indonesia
[4] Department of Civil Engineering, University of South Africa, Pretoria 1709, South Africa

Corresponding Author Email: agarwala.cst@rub.edu.bt

https://doi.org/10.18280/ijht.430204

Received: 18 November 2024
Revised: 16 March 2025
Accepted: 1 April 2025
Available online: 30 April 2025

Keywords:
pipeline flow, erosion dynamics, Tabakoff model, Finnie model, slurry transport, CFD

ABSTRACT

The transportation of fluids in pipelines containing solid impurities poses significant challenges due to the risk of erosion and material degradation, particularly in complex flow conditions. This study examines the erosion behavior in an L-shaped pipeline using Computational Fluid Dynamics (CFD) with the ANSYS CFX simulation package. The investigation evaluates two erosion models, Finnie and Tabakoff, under varying fluid velocities to assess their predictive capabilities. Results highlight that the Tabakoff model, which considers particle impact velocity, predicts higher erosion rates, emphasizing the critical influence of particle size and velocity on pipeline integrity. Turbulence modeling comparisons reveal that the k-ω model provides superior accuracy in predicting near-wall turbulence and erosion rates, especially at critical velocities ranging from 4.8 m/s to 5.8 m/s, where erosion risks are heightened. The study also identifies significant turbulent pressure impulses as key contributors to material wear. These findings offer valuable insights for optimizing pipeline design, material selection, and operational strategies to enhance the durability and reliability of fluid transport systems across various industrial applications. The findings underscore the necessity of selecting appropriate erosion models and turbulence formulations to ensure accurate predictions. This study provides a framework for mitigating erosion through optimized design and operational strategies, enhancing pipeline longevity in particle-laden flows.

1. INTRODUCTION

Erosion in pipeline systems poses a significant challenge to the integrity and reliability of fluid transport networks, affecting various industries, including oil and gas, water supply, and chemical processing [1]. These systems are exposed to a variety of potentially inconsistent flow conditions (i.e. pressure, velocity, solid impurities), and the resulting complex mechanisms are responsible for the erosion [2]. The understanding of these mechanisms is important to develop effective maintenance protocols and novel design strategies for maintaining the longevity of pipeline infrastructure [3]. Over the past several years there has been a significant emphasis on pipeline integrity tied to increasing incidences of failures caused by erosion and corrosion. Therefore, a pressing need exists for all-encompassing investigations and explanations of the fundamental processes of erosion as well as solutions to mitigate the effects [4]. The focus of this study is to investigate erosion rates in pipeline systems under particle-laden flow conditions and the combined effects of fluid dynamics and particle interactions. This study bridges some of the knowledge gaps and provides actionable insight into how to optimize pipeline designs by examining various modeling approaches such as those of Finnie [5] and Tabakoff et al. [6]. Ultimately, the aim is to minimize erosion and optimize the operational longevity of pipelines for safer and more efficient fluid transport systems.

1.1 Erosion mechanisms in pipeline systems

The fluid transport through the pipelines is a complex operation that includes the effect of bends, inclinations, and the presence of solid impurities. According to research conducted by Zhang et al. [7], sand particle impact on the pipeline wall depends on the shape of the particles, velocity, diameter, and geometry of the pipeline. The results of their analysis indicate that bent parameters and the continuous pipeline characteristics can critically affect the erosion and wear mechanisms, characterizing particles as a decisive contributor to wear in curved pipelines. Wang and Zheng [8] further highlight the need for an understanding of critical flow velocities in understanding erosion-corrosion phenomena. The review recommends ways to determine these velocities in the presence of surface films on metal surfaces (such as passive

films or corrosion products). It is necessary for predicting the behavior of erosion in pipelines under different flow conditions. In addition, Liu et al. [9] also describe erosion corrosion features of X80 pipeline steel under applied angles of attack in two-phase flow impingements. This finding suggests that erosion rates are affected by flow dynamics so that the weight loss of samples increases with a decrease in the im-pact angle. As critical factors affecting operational costs, variations of erosion-corrosion resistance of steel pipes used in oil sand operations are addressed by Chung et al. [10]. The results of this analysis provide an additional understanding of the economic impact of erosion and corrosion in pipeline systems.

1.2 Impact of fluid dynamics on erosion rates

Li et al. [11] have found that the distribution of fluid velocity at bends may have a considerable impact on erosion rates in pipeline systems. The findings are consistent with Wang et al. [12] who investigate the directional effects of flow on particle erosion, and provide valuable insight into the dynamics of particle-laden flows. Othman et al. [13] identified fluid flow parameters that impact erosion rates, showing that changes in flow velocity led to dramatic differences in the erosion landscape. Yu et al. [14] summarize the strategies for managing the fluid-solid erosion wear in pipelines either modeling, detecting, resisting, or taking a risk. This review covers theoretical and applied research on pipeline erosion and makes suggestions about future coping strategies.

1.3 Erosion monitoring and mitigation innovations

Improved pipeline integrity monitoring techniques and mitigation strategies are necessary given recent advancements. The work of Balasubramanian et al. [15] and Xu et al. [16] emphasizes the need for novel erosion detection methods and the development of successful mitigation strategies. Li et al. [17] use particle image velocimetry (PIV) to characterize the velocity particle conditions of compressor blade materials via a Finnie wear model which is parameterized. Moreover, Teran et al. [18] point out the importance of integrated modeling approaches to predict the wear behavior of components subjected to simultaneous cavitation and hard particle erosion due to synergistic effects. Additionally, Wee and Yap [19] utilize CFD based on an Eulerian-Lagragian approach to study sand erosion behavior in pipelines, revealing the complicated coupling between fluid dynamics and solid particle impacts. Rahimi-Larki et al. [20] also suggest a coupled CFD method to simulate erosion in cohesive materials and show how advanced modeling can be applied to a wide range of geometries.

1.4 Erosion dynamics and modeling approaches

Most of the studies have been focused on the mechanism of erosion and the determining parameters of erosion behavior. Erosion behaviors under various parameters like flow velocity, particle diameter, and rotation are examined by Veiskarami and Saidi [21]. The work emphasizes the intricacies of erosion dynamics and demonstrates the need for multiple modeling approaches to encompass these interactions. The pioneering research of Finnie [5] and Tabakoff et al. [6] laid the foundation for models predicting erosion caused by solid particle impacts on walls. These studies are further elaborated by Zhang et al. [22], which further emphasizes the application of these models to the prediction of erosion in pipeline applications. The Finnie model is preferred for its simplicity and low computational cost, while the Tabakoff model makes a more detailed Erosion dynamics representation, but at higher complexity. The Finnie model is based on material wear due to low-angle particle impacts, making it suitable for gradual erosion analysis, particularly in brittle materials. However, it does not fully account for the effects of high-velocity particle impacts. The Tabakoff model, on the other hand, explicitly considers both particle speed and impact angle, making it more effective in predicting erosion under high-velocity conditions, such as those found in pipeline bends where particles experience significant directional changes. By employing both models, a more comprehensive understanding of erosion mechanisms is achieved. Our study is particularly relevant for this dual model approach because it enables a full understanding of the erosion phenomena under different conditions and potentially leads to better predictive capabilities. Okafor and Ibeneme [23] simulated erosion along pipes of varied geometry and showed that the shape of the pipe plays a major role in the severity of erosion. This additional supports our approach to optimize pipeline design as well as mitigating pipeline erosion in critical areas using the combined Finnie and Tabakoff models. Zhang et al. [24] further engage in this discourse by calibrating the parameters of the erosion models using a Newton iteration method, validating it with computational fluid dynamics (CFD) simulations. The correlations found between value-predicted erosion and experiment further support the necessity of a dual modeling approach in our work. Nevertheless, significant gaps remain in the understanding of the counteracting effects of geometry and fluid dynamics on erosion rates. Previous studies have rarely looked at these factors individually, rather than their combined effect. To fill these gaps, this study explores optimized geometric designs and tailored mitigation strategies and helps to contribute to the development of more resilient pipeline systems. It is hypothesized that pipeline design can be optimized on both the basis of fluid velocity and particle dynamics, which would result in a significant reduction in erosion rates. To guide the investigation, the following research questions have been formulated:

•What are the effects of fluctuations in fluid velocity and particle size on erosion rates of pipeline systems?

•How do geometric characteristics of pipelines affect the distribution and severity of erosion in high-velocity conditions?

•How do these conditions compare in the accuracy and applicability between the Finnie and Tabakoff erosion models?

During the fluid flow process, the particles in the fluid impact the wall of the tube (or pipe), causing erosion, especially at higher velocities. In order to predict the wear of materials during the fluid flow process, it is essential to incorporate erosion models. With the use of the erosion model, we can predict material loss and identify zones of structural degradation. To further understand the erosion mechanisms in piped flow systems, these research questions need to be addressed. If pipeline failures have large financial and environmental consequences, effective mitigation strategies must be identified. The fluid flow characteristics and erosion rates in L-shaped pipelines carrying fluids with inherent impurities are evaluated using Computational Fluid Dynamics (CFD) through the ANSYS CFX simulation package. This

study presents a comparative analysis of two existing erosion models, Finie and Tabakoff, and provides a basis for examining the applicability and inapplicability of these same models within the context of fluid flows containing solid particles. The research also explores the impact of pipe bend geometry on the severity of the erosion. This study provides new insights into the interaction between fluid dynamics and erosion mechanisms, which will facilitate designing for optimum pipeline designs and improve their integrity and longevity under high-stress conditions.

2. MATERIALS AND METHODS

In this study, advanced CAD design combined with CFD simulations and erosion modeling methodology is used to provide an integrated approach to evaluating the effect of particle-laden flow on pipeline erosion. The steps outlined below ensure precise geometric representation, effective boundary condition setup, and a thorough comparative analysis of erosion mechanisms using two distinct models: Finnie and Tabakoff. The methodology process encompasses modeling of an L-shaped (900) pipeline bend in Creo design software. The Creo is sketch-based, parametric 3D modeling software that facilitates complex 3D modeling of pipe bends. The Creo 6.0 software has unique tools for pipeline design i.e. sketch and sweep [25, 26].

2.1 Geometric modeling

The first step is to generate a 3D geometric model of the L-shaped pipeline bend with Creo Parametric, one of the most capable and comprehensive, sketch-based parametric CAD software. Parametric design capability enables flexibility and precision in design as the software mimics real-world pipeline structures. Figure 1 shows the modeled pipeline bend with both length and height of 15 meters each [27]. The choice of geometry is motivated by typical industrial pipeline configurations seen in practice. After that, the Creo 6.0 model was exported to ANSYS for additional simulation to enable seamless integration between the CAD and simulation environment. The imported design of the pipeline is shown in Figure 1.

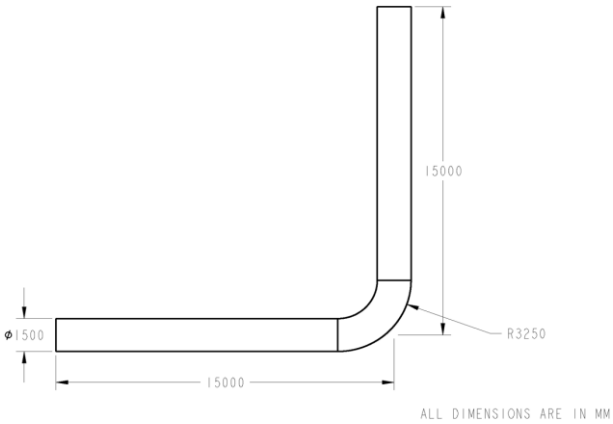

Figure 1. Imported CAD model of pipeline

2.2 Importing and meshing in ANSYS

The subsequent step after meshing is discretization. The pipeline model was then exported to ANSYS Design Modeler software where meshing took place. Accurate numerical solutions require a good meshing that is essential for the degradation of complex geometry into smaller elements [28]. The selection of these parameters was based on a balance between computational efficiency and accurate representation of boundary layer effects close to the walls where erosion is most severe [29]. For meshing, the element sizing is set to 11mm and a growth rate of 1.1. The inflation is set to smooth transition type and the transition ratio is set to 0.77. After specifying mesh settings, the model is meshed. The discretized model of the pipeline is shown in Figure 2. The model contains 762675 elements and 880492 nodes.

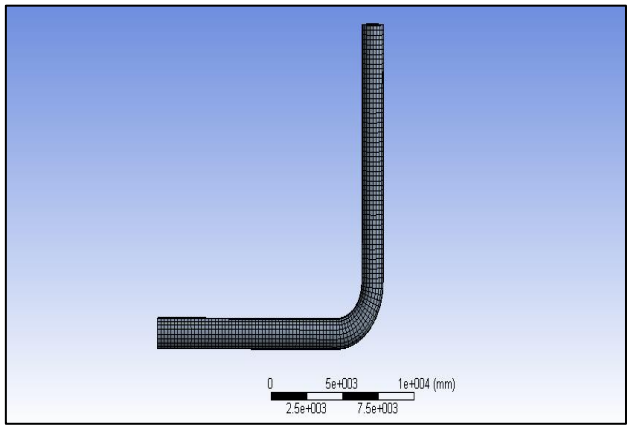

Figure 2. Meshed model pipeline

2.3 Material properties and boundary conditions

The fluid material is oil and the solid particles defined is slurry. Table 1 presents the properties of the fluid (oil) and particles (slurry) to be used in the simulation of this study. These values are chosen to represent the most common features of particle-laden flows encountered in industrial pipelines so that the study stays highly applicable. To capture arrange of operational conditions, different particle sizes were tested: 110 µm, 150 µm, and 200 µm respectively. These sizes were selected so that the impact of having different dimensions of particles on erosion rates could be determined.

Table 1. Material property of fluid [26]

Property	Value
Density (Kg/m^3)	1850
Kinematic Viscosity (mPa.s)	840
Solid concentration (wt %)	55%
Particle size	110 µm, 150 µm and 200 µm

After discretization, the model is applied with fluid flow boundary conditions. The fluid flow boundary conditions include domain definition, inlet boundary conditions, and outlet boundary conditions. The domain type defined for the model is fluid with particle transport solid as mentioned earlier.

2.3.1 Inlet boundary conditions

The velocity profile was prescribed at the inlet (green colored) as 3.8 m/s and the turbulence intensity was further exerted at 5% as shown in Figure 3. These values are characteristic of normal operating conditions in pipelines and help provide a realistic approximation to actual fluid behavior.

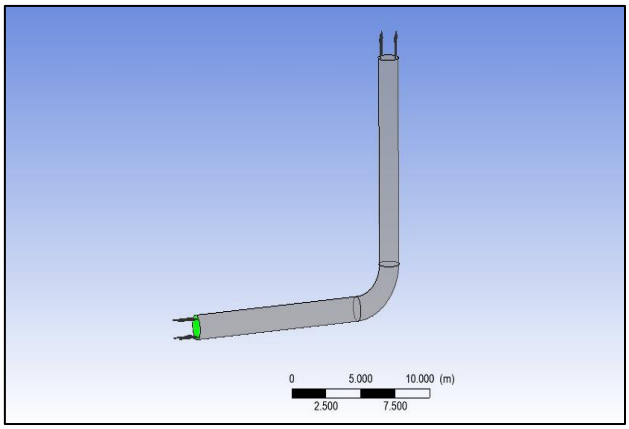

Figure 3. Fluid inlet boundary condition

2.3.2 Outlet boundary conditions

At the outlet, a 0 Pa pressure difference was applied comparing the pressure of the pipe with the atmospheric pressure in order to resemble the free-flowing exit condition as shown in Figure 4. This configuration allows for precise replicating of the pressure gradient that drives the flow to mimic most industrial pipeline conditions. The fluid transport type of the domain was described by the particle transport. The solid particles represent slurry which is a typical material to be transported through pipelines in oil & gas fields.

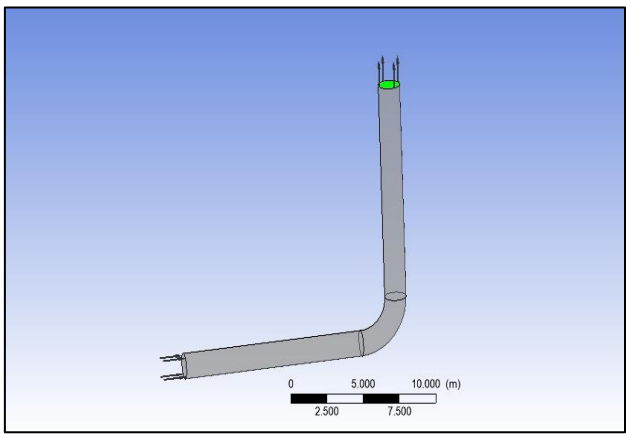

Figure 4. Fluid outlet boundary condition

2.4 Finnie and Tabakoff -erosion models

The two erosion models utilized in this research are Finnie and Tabakoff as explained in Section 1 to analyze both gradual and severe erosion mechanisms in pipelines. The first set of simulations is based on the Finnie model, which can reliably predict wear in brittle materials at low-impact angles, and simulate gradual wear in a few selected pipeline sections. It is however limited in the effectiveness of capturing complex interactions in the high particle velocities or larger sizes. The second set of simulations uses the Tabakoff model that includes impact velocity angles and is formulated for high-velocity particles that deform the material significantly as in pipeline bends. This comparative approach helps understand different erosion mechanisms that must be improved to enhance pipeline reliability and functionality. Combining both models creates a robust framework to assess erosion behavior under a range of operational conditions that is necessary to extend pipeline longevity and avoid pipeline failures caused by material erosion. Geometric modeling through Creo Parametric for precision and flexibility, and mesh generation and CFD simulation using ANSYS to make predictions of erosion with accuracy. The Finnie and Tabakoff models were specifically selected for their complementary nature—Finnie typically offers efficient predictive efficiency for low velocity, shallow angle erosion, while Tabakoff provides meaningful insight into severe conditions for a wide spectrum of pipeline erosion cases.

2.5 Governing equations

For this study, several governing equations are used to accurately describe the fluid dynamics. For incompressible fluid problems, where density is unchanged (Constant), the continuity Eq. (1) becomes important, ensuring a constant flow rate [30].

$$\partial\rho/\partial t+ \nabla(\rho u)=0 \quad (1)$$

Typically, the Navier Strokes (momentum equation) are solved using a turbulence model like the standard (k−ϵ, k−ω). In incompressible form [31], the momentum Eq. (2) is:

$$(\partial(\rho v))/\partial t+\nabla(\rho vv)=-\nabla p+\nabla.(\mu\nabla v)+\rho g+F \quad (2)$$

k-ϵ (3) and k-ω (4) turbulence models are also employed. The turbulent kinetic energy is given by [32].

$$(\partial(\rho k))/\partial t+ \nabla (\rho ku)= \nabla+\nabla.(\mu_t/\sigma_k\nabla k)+G_k+\rho\epsilon \quad (3)$$

$$(\partial(\rho k))/\partial t+\nabla(\rho kv)=P_k-\beta^*\rho k\omega+\nabla.[(\mu+\sigma_k\mu_t)\nabla k] \quad (4)$$

The Finnie erosion model is based on the assumption that erosion is primarily caused by slurry particles impinging surfaces at low-impact angles [33]. The Finnie erosion rate (5) is given by:

$$dM/dt=C\ .m\_p.v^2.f(\theta).N \quad (5)$$

In the case of the Tabakoff erosion model, the effect of both normal and tangential velocity components is considered [33]. The model accounts for the cumulative mass loss rate (6).

$$dM/dt=K.m_p.(v_n)^n.(v_t)^t.(\cos\theta)^p.N \quad (6)$$

2.6 Solver settings and simulation parameters

After applying fluid flow boundary conditions, the solver settings are defined for the model as shown in Table 2. The upwind interpolation is set to double precision type and the advection scheme is set to high resolution. The RMS residual target for the analysis is set to .000001. The total iterations defined for the simulation is set to 1000. These choices maintain simulation stability and reliability, especially with high turbulence near the elbow region of the pipeline. For CFD simulation, the time step selected is $\Delta t = 0.001$s which is based on Courant-Friedrichs Lewy (CFL) condition. At this time step, the tradeoff is achieved between stability, accuracy as well as computational efficiency. The total simulation time for the analysis is 3.5 secs and erosion effects started to be evident after 1.6 secs. The “Semi-Implicit Method for Pressure Linked Equations (SIMPLE)” algorithm was selected for pressure velocity coupling which facilitates stable convergence in each

iteration [34]. The RMS residual target is set for the simulation which is set to 1e-5 for each time step and provides accurate results.

Table 2. Summarized conditions for simulation

Parameter	Value
Inlet speed	3.8 m/s
Outlet pressure	0 Pa
Erosion Model	Finnie erosion and Tabakoff
Turbulence intensity	5%
Turbulence model used	K epsilon
RMS residual	0.000001

The applied methodology uses well-defined boundary conditions and high-precision solver settings enabled by ANSYS to produce accurate and reliable results. The analysis is relevant to the many industries with erosion problems by testing a wide range of particle sizes and flow velocities. The combination of the Finnie and Tabakoff models allows for a holistic view of erosion mechanisms, involving both gradual wear and high impact case. The standard turbulence models were chosen to simulate flow behavior in turbulent regions and thus increase the accuracy of particle interaction with pipeline walls. This approach satisfies the research objectives and provides insights for pipeline design and optimization that are susceptible to erosion by particle-laden flows.

3. RESULTS

The contour plots of velocity, pressure, and erosion rates are then collected from the CFD simulations with various fluid velocities and turbulence models. The results are presented in two main sections: The first are simulations with the Finnie erosion model; the second the simulations with the Tabakoff erosion model. The performance of the k-ε, RNG k-ε, and k-ω turbulence models are compared for each erosion model as well.

3.1 Finnie erosion model results

3.1.1 Velocity plots at different speeds using the Finnie erosion model

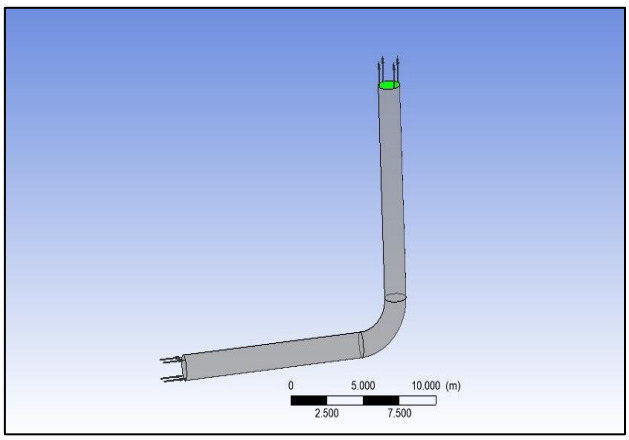

Figure 5. Velocity plot at 3.8 m/s

In the 1st case, the analysis uses the Finnie erosion model. The analysis is conducted at different fluid speeds i.e., 3.8 m/s, 4.85 m/s, and 5.8 m/s. The velocity plot at 3.8 m/s is shown in Figure 5. The plot shows higher velocity at the pipe bend corner. The magnitude of velocity at the bend is 4.68 m/s. The velocity of the fluid is lesser on the opposite corner of the tube with a magnitude of 2.47 m/s.

The velocity plot at 4.8 m/s is shown in Figure 6. The plot shows higher velocity at the pipe bend corner. The magnitude of velocity at the bend is 6.26 m/s. The velocity of the fluid is lesser on the opposite corner of the tube with a magnitude of 2.79 m/s.

The velocity plot at 5.8 m/s is shown in Figure 7. The plot shows higher velocity at the pipe bend corner. The magnitude of velocity at the bend is 7.57 m/s. The velocity of the fluid is lesser on the opposite corner of the tube with a magnitude of 3.37 m/s.

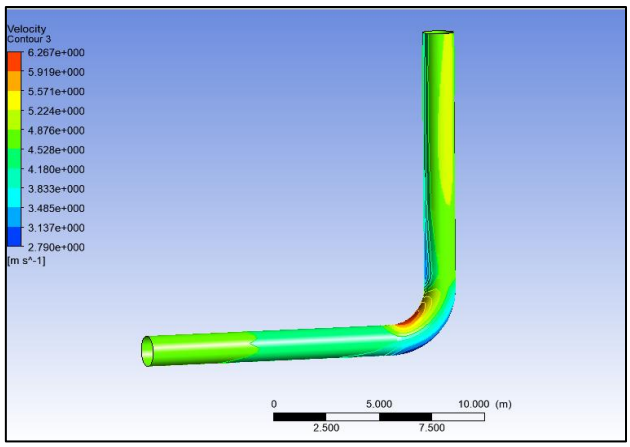

Figure 6. Velocity plot at 4.8 m/s

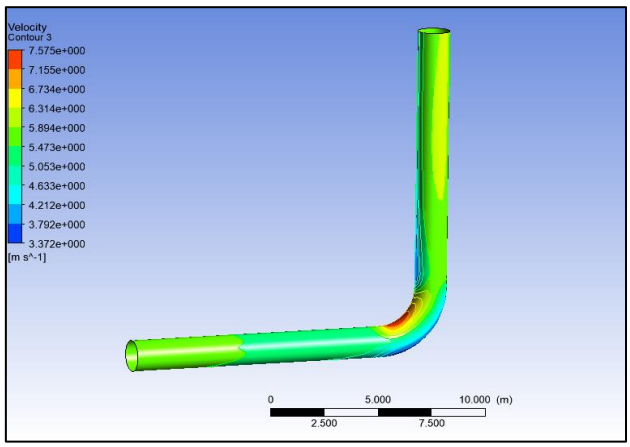

Figure 7. Velocity plot at 5.8 m/s

3.1.2 Erosion rate density plots using Finnie erosion model

As the fluid flows through the pipe, the slurry particles impact the pipe wall causing it to erode. The erosion rate density plot is obtained for the pipe as shown in Figure 8. The zones with the highest erosion rate correspond to the region where slurry particles impact the pipe wall. The erosion rate is uniform for all other zones of the pipe with a magnitude of 0.576 Kg/m^{2}s.

The erosion rate density plot is obtained for the pipe for fluid flowing at 4.8 m/s as shown in Figure 9. The erosion rate is higher at the tube where fluid enters with a maximum magnitude of 5.71 Kg/m^{2}s as represented by red-colored zones.

The erosion rate density plot is obtained for the pipe for fluid flowing at 5.8 m/s as shown in Figure 10. The erosion

rate is higher at the tube where fluid enters with a maximum magnitude of 8.2 Kg/m^{2}s as represented by red-colored zones.

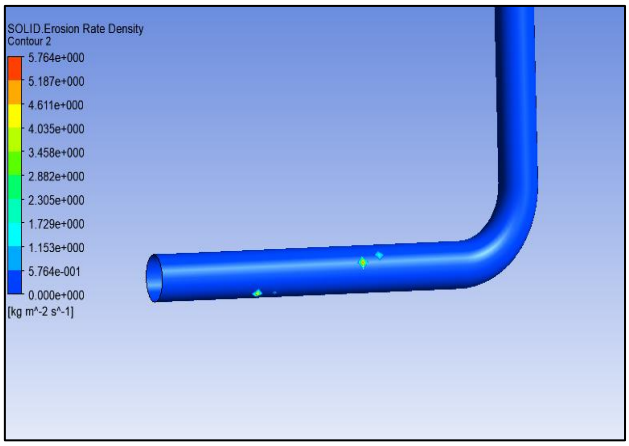

Figure 8. Erosion rate density plot at 3.8 m/s

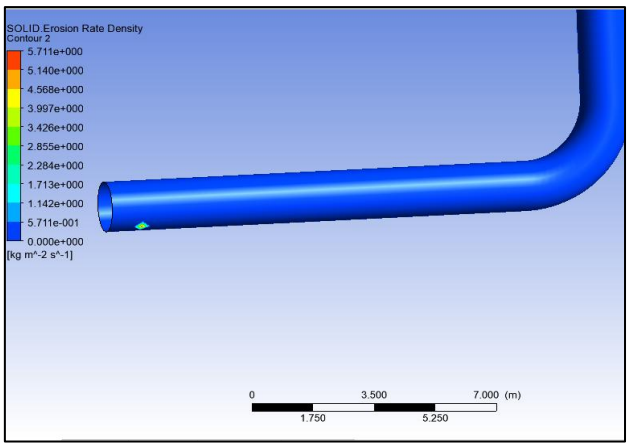

Figure 9. Erosion rate density plot at 4.8 m/s

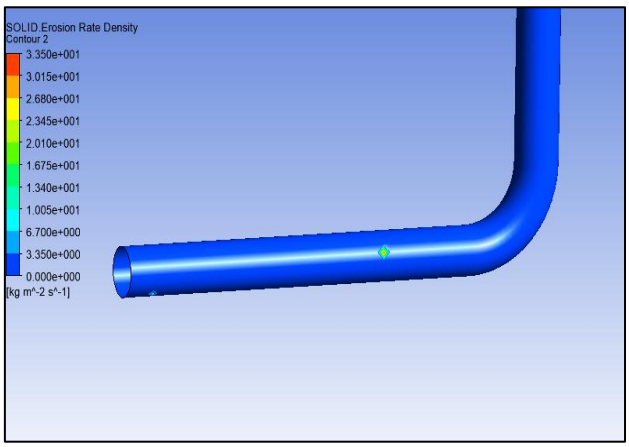

Figure 10. Erosion rate density plot at 5.8 m/s

3.1.3 Pressure distribution using the Finnie erosion model

The pressure variation plot is generated for the pipeline as shown in Figure 11. The pressure is maximum at the corner of the tube. The pressure on the outer surface is the compressive type with a magnitude of 3164 Pa and is tensile on the inner surface of the tube. The pressure at this zone is 5670 Pa as represented by a dark blue colored zone.

The pressure variation plot at 4.8 m/s is generated for the pipeline as shown in Figure 12. The pressure is maximum at the corner of the tube. The pressure on the outer surface is com- a pressure type with a magnitude of 6599 Pa and is tensile on the inner surface of the tube. The pressure at this zone is 9062 Pa as represented by a dark blue colored zone.

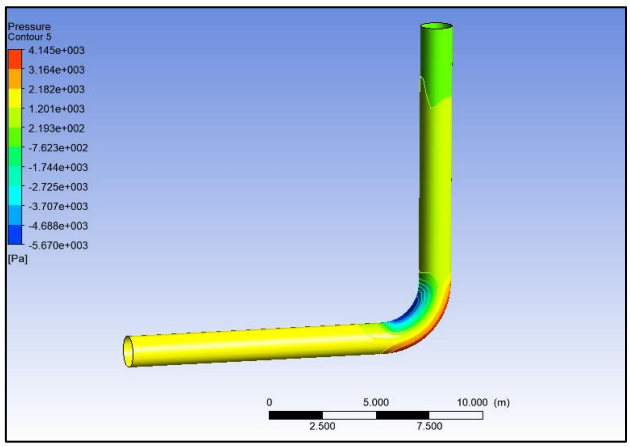

Figure 11. Pressure distribution plot at 3.8 m/s

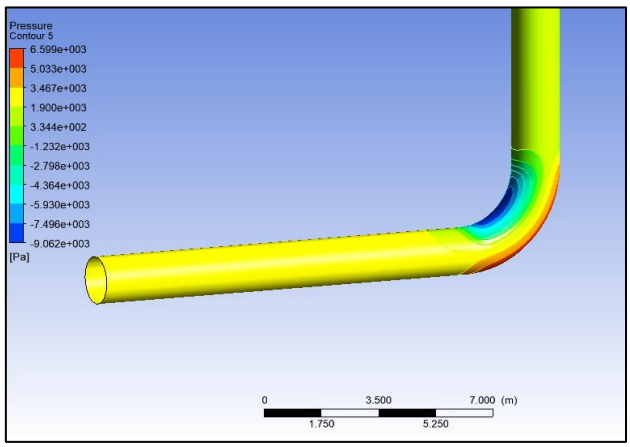

Figure 12. Pressure distribution plot at 4.8 m/s

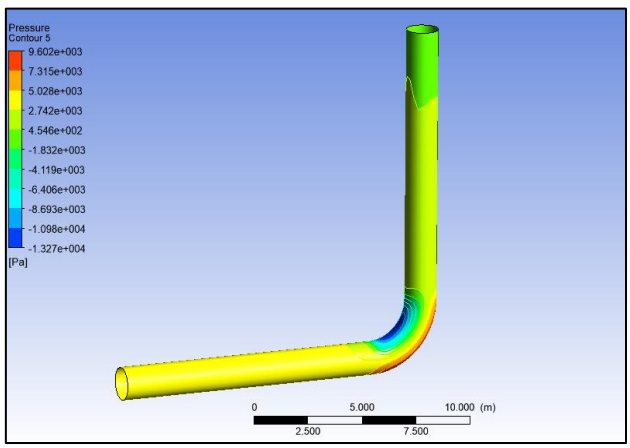

Figure 13. Pressure distribution plot at 5.8 m/s

The pressure variation plot at 5.8 m/s is generated for the pipeline as shown in Figure 13. The pressure is maximum at the corner of the tube. The pressure on the outer surface is the compressive type with a magnitude of 9602 Pa and is tensile on the inner surface of the tube. The pressure at this zone is 1327 Pa as represented by a dark blue colored zone.

3.2 Tabakoff erosion model results

The next set of analyses is conducted using the Tabakoff turbulence model. From the analysis, the erosion rate density, pressure distribution, and velocity plots are generated for the pipeline.

3.2.1 Velocity plots at different speeds using Tabakoff erosion model

The velocity distribution plot at 3.8 m/s inlet speed is generated for the Tabakoff erosion model as shown in Figure 14.

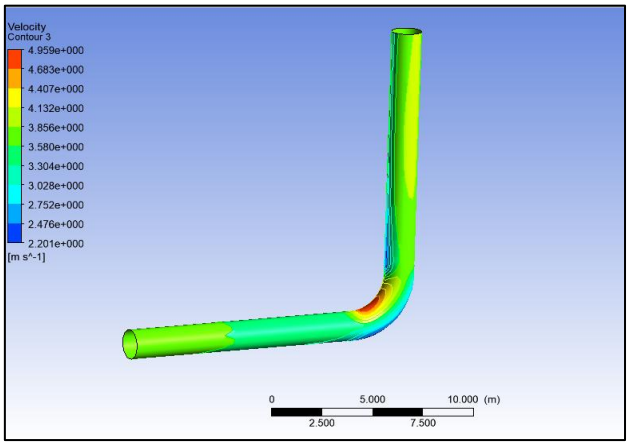

Figure 14. Velocity distribution plot at 3.8 m/s

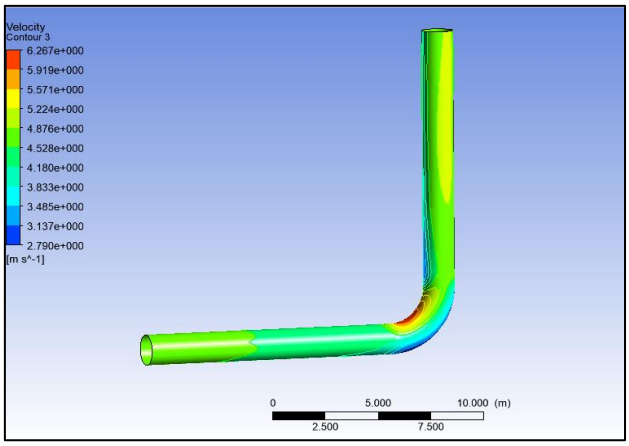

Figure 15. Velocity distribution plot at 4.8 m/s

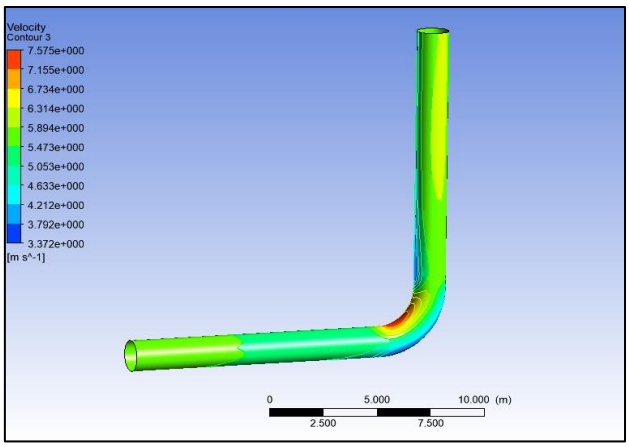

Figure 16. Velocity distribution plot at 5.8 m/s

The plot shows higher velocity at the pipe bend corner. The magnitude of velocity at the bend is 5.03 m/s. The velocity of the fluid is lesser on the opposite corner of the tube with a magnitude of 2.72 m/s. At 4.8 m/s, the magnitude of velocity at the bend is 6.04 m/s. The velocity of the fluid is lesser on the opposite corner of the tube with a magnitude of 3.7 m/s as shown in Figure 15.

At 5.8 m/s, the fluid velocity at the pipe bend is maximum and there is induced turbulence flow at this zone. The fluid velocity at the pipe bend inner surface is 6.42 m/s as depicted by red colored region in Figure 16, whereas the fluid velocity on the opposite corner of the pipe is 3.65 m/s.

3.2.2 Erosion rate density plots using Tabakoff erosion model

As the fluid flows through the pipe, the slurry particles impact the pipe wall causing it to erode. The erosion rate density plot is obtained for the pipe using the Tabakoff erosion model as shown in Figure 17.

The zones with the highest erosion rate correspond to the region where slurry particles impact the pipe wall. The maximum erosion rate for the Tabakoff erosion model is represented by a colored spot where the erosion rate is 5.93 kg/m^2s. At 4.8 m/s, the pipeline exhibited 2 zones of maximum erosion rate density (Figure 18) which is represented by two colored spots.

The erosion rate at these two zones ranges from 12.29 Kg/m^2s to 19.38 Kg/m^2s. These two zones are most susceptible to crack initiation during the operational phase. At 5.8 m/s, the maximum erosion rate is obtained near the pipeline end as represented by yellow and red colored regions in Figure 19.

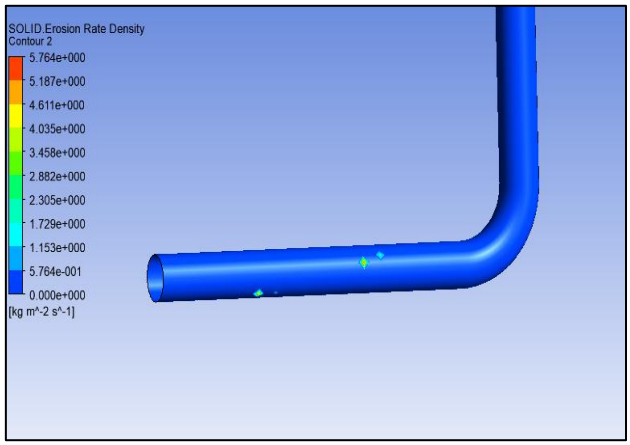

Figure 17. Erosion rate density at 3.8 m/s

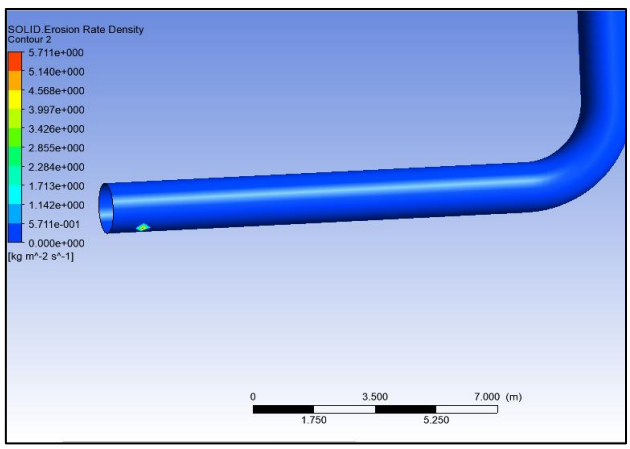

Figure 18. Erosion rate density at 4.8 m/s

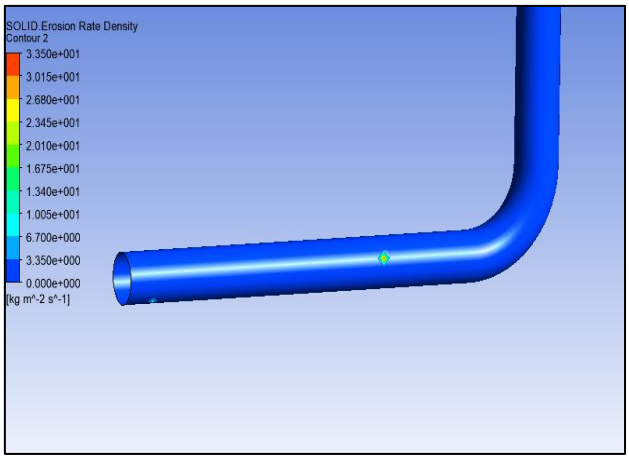

Figure 19. Erosion rate density at 5.8 m/s

The erosion rate density at this zone is nearly 5.58 Kg/m^{2}s. It is evident that at this fluid speed, the pipeline near the fluid outlet is more susceptible to damage by crack initiation.

3.2.3 Pressure distribution plots using Tabakoff erosion model

The pressure variation plot with the Tabakoff erosion model obtained at 3.8 m/s is generated for the pipeline as shown in Figure 20. The pressure is maximum at the corner of the tube. The pressure on the outer surface is the compressive type with a magnitude of 3803 Pa and is tensile on the inner surface of the tube.

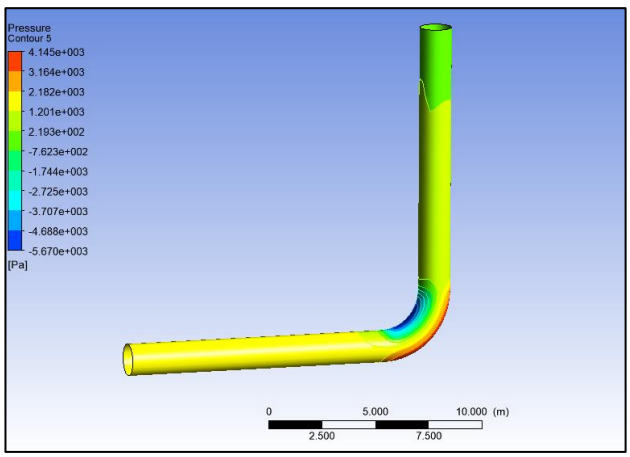

Figure 20. Pressure distribution plot at 3.8 m/s

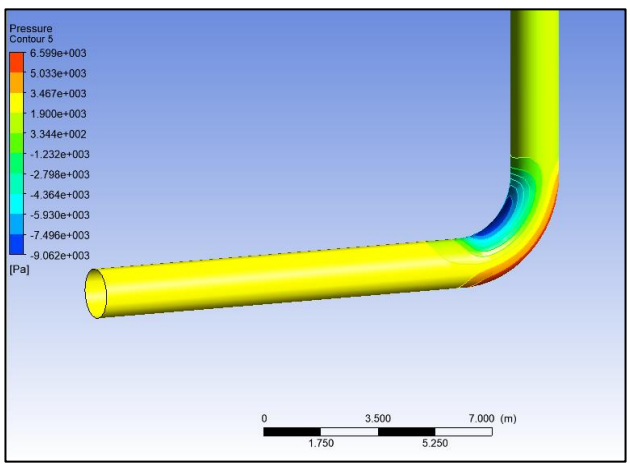

Figure 21. Pressure distribution plot at 4.8 m/s

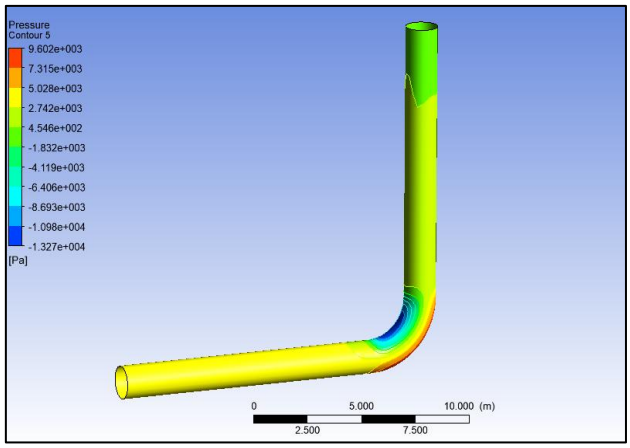

Figure 22. Pressure distribution plot at 5.8 m/s

The pressure at this zone is 6023 Pa as represented by a dark blue colored zone. The pressure variation plot with the Tabakoff erosion model obtained at 4.8 m/s is generated for the pipeline as shown in Figure 21.

The pressure is maximum at the corner of the tube. The pressure on the outer surface is the compressive type with a magnitude of 6057Pa and is tensile on the inner surface of the tube. The pressure at this zone is 8054Pa as represented by a dark blue colored zone. The pressure variation plot with the Tabakoff erosion model obtained at 5.8 m/s is generated for the pipeline as shown in Figure 22.

The pressure is maximum at the corner of the tube. The pressure on the outer surface is the compressive type with a magnitude of 6834 Pa and is tensile on the inner surface of the tube. The pressure at this zone is 7326 Pa as represented by a dark blue colored zone.

3.3 Comparison of turbulence models

3.3.1 k-ε, RNG k-ε, and k-ω models

Each turbulence model is analyzed in terms of erosion rate density and pressure prediction for both the Finnie and Tabakoff erosion models:

k-ε model

In CFD, the k epsilon turbulence model is ideal for simulating fully developed turbulence, events such as that of flow through pipes. It is evident from the results that the erosion rate density increases as the fluid velocity increases. The turbulence model determines how the flow interferes with the pipeline's walls in case of erosion. The k epsilon turbulence model also assumes that the turbulence is isotropic and therefore the eddy viscosity in the whole flow field is the same. This assumption is generally acceptable when the flow in the pipeline is fully developed and in the fully turbulent zone, but it can give underestimated anisotropy of turbulence in the zones of flow separation or the vicinity of the wall. The turbulence intensity predicted by the model is higher in regions of higher turbulence which results in higher particle impingement velocities and hence higher erosion. The k-ε model is used to estimate pressure fluctuations and flow separation in pipelines particularly in areas such as pipe bends. The model is applicable for the pressure surge in the high turbulence zones as a result of localized enhancement of erosion rate density. Nevertheless, one of the most significant limitations of the k-ε model for turbulent modeling is the assumption of isotropy that leads to a very small

underestimation of the pressure near wall-bounded areas where anisotropic turbulence is more dominant as indicated in Table 3.

Table 3. Finnie erosion model using *k* epsilon turbulence model

Fluid Velocity	Erosion Rate Density (Kg/m^2s)	Maximum Induced Pressure (Pa)
3.8 m/s	5.76	5670
4.8 m/s	6.26	6599
5.8 m/s	8.28	9602

In the case of the Tabakoff erosion model, the erosion rate density increases with the increasing fluid velocity as is common with slurry or particulate-laden flows where the particles impact and abrasive action on the pipe wall as indicated in Table 4.

Table 4. Tabakoff erosion model using k epsilon turbulence model

Fluid Velocity	Erosion Rate Density (Kg/m^2s)	Maximum Induced Pressure (Pa)
3.8 m/s	11.88	8832
4.8 m/s	21.53	9845
5.8 m/s	24.4	11548

The Tabak off erosion model takes into consideration the particles that are expelled onto the surface and therefore is very much dependent on velocity differences: Higher erosion rates are found even at moderate fluid velocities of 3. 8 m/s and the erosion rate density begins from a relatively higher value of 11.88 kg/m^2s. This implies that the particles in flow have a large impact energy to cause material loss from their wall. It can be deduced that the sharp increase in erosion rate density from 11.88 kg/m^2s to 21.53 kg/m^2s between 3.8 m/s and 4.8 m/s, shows the nonlinear dependency of velocity for the erosion in the Tabakoff model which depends on the impact angle of particle, velocity of particle and size of the particle. At 5.8 m/s it is seen that the rate of increase is slowing down, though the value is high at 24.4 kg/m^2s. This indicates that at extremely high velocities, one gets to a point where particle impact frequency is very high hence additional velocity enhancement has the least impact on further raising erosion. The k-ε turbulence model represents the mass turbulent flow field but is less precise at the region near the wall compared to finer models (e.g., k-ω). But it indicates the relationship between the flow velocity and erosion that even at this level the flow velocity is high and so is the erosion. This would be mainly attributed to the fact that at high velocities, there is a high kinetic energy associated with the particles in the flow thus resulting in high energy impacts on the pipe wall.

RNG k-ε model

As it's evident in Table 3, the erosion rate density rises steadily with increasing fluid velocity. The RNG k-ε model analyzes the relationships for the interaction of the turbulent flow and solid particles in the flow direction and determines the dependence of the erosion mechanisms for different velocities. The increase in the erosion rate density is due to the increased velocity of slurry particles that cause more frequent and forceful impacts of slurry particles with the pipeline wall particularly in regions of high turbulence according to the observed RNG k – ε model. The RNG k-ε model explains the eddies and variations in the turbulent flow and more so in zones whereby flow detachment or swift alteration in direction may be observed such as bends or junctions in a pipeline.

It also shows that an increase in turbulent energy at larger velocities causes higher erosion rates due to the stronger impact of particles with the wall than the results obtained using the standard k-ε model. Thus, the RNG k-ε model provides a more accurate estimate of near-wall flows, and so, the rates of particle erosion are correspondingly higher. This is of particular significance in less fluid flow velocity areas of the pipeline in which the potentials of particle impact on the pipe wall are higher. The RNG k-ε model performs significantly better in the prediction of the flow separation e. g. in pipe bends and thus provides better estimates of erosion rates in such an area. When particles are entrained in the separated flow, they are all forced into the regions of recirculation and hence generate higher wall impacts implying that erosion is higher. Table 5 shows the values obtained using the Finnie erosion model using the RNG k epsilon turbulence model.

Table 5. Finnie erosion model using RNG k epsilon turbulence model

Fluid Velocity	Erosion Rate Density (Kg/m^2s)	Maximum Induced Pressure (Pa)
3.8 m/s	6.14	5670
4.8 m/s	6.70	6599
5.8 m/s	8.84	9602

The erosion rate density is also significantly higher than the ones obtained from the standard k-ε model for all velocities. The pressure prediction by the RNG k-ε model is higher than that of the k epsilon turbulence model. This behavior reflects better handling of high turbulence zones by the RNG k-ε model especially for intense pressure fluctuation. Table 6 shows the values obtained from the Tabakoff erosion model.

Table 6. Tabakoff erosion model using RNG k epsilon turbulence model

Fluid Velocity	Erosion Rate Density (Kg/m^2s)	Maximum Induced Pressure (Pa)
3.8 m/s	12.52	8972
4.8 m/s	22.32	10051
5.8 m/s	25.24	11802

The erosion rate density and maximum induced pressure resulting from the application of the RNG k-ε turbulence model and the Finnie and Tabakoff erosion models to the fluid velocities of interest are presented in Tables 4 and 5 respectively. Table 4 shows the Finnie model with a gradient increase in erosion rate density from 6.14 kg/m^2s to 8.84 kg/m^2s as the flow rate increases from 3.8 m/s to 5.8 m/s, and a rise in maximum induced pressure from 5670 Pa to 9602 Pa.

These results indicate that the Finnie model represents the behavior of erosion at lower impact angles but may overestimate the influence of increased particle velocity. However, Table 5 reveals that the Tabakoff model yields much greater erosion rates, even as low as 12.52 kg/m^2s at 3.8 m/s and up to 25.24 kg/m^2s at 5.8 m/s, with maximum pressures running up from 8972 Pa to 11802 Pa. The Tabakoff model's ability to account for impact angle and thus higher particle dynamics enhanced its capability to model aggressive erosion in high-velocity flows.

k-ω model

The k-ω model excels in capturing boundary layer effects, making it particularly useful for erosion prediction in pipelines carrying slurries. Turbulent kinetic energy is accurately modeled near the wall, leading to a better understanding of particle impacts. The k-ω model's focus on near-wall flow means it provides precise predictions for erosion where particles interact directly with the pipeline walls. This is particularly important in cases where flow separation occurs, such as bends or elbows in the pipeline, where particles deviate from the main flow and impact the wall more frequently. At high velocities, like 5.8 m/s, the erosion rate density and induced pressure increase substantially as shown in Table 7.

Table 7. Finnie erosion model using k-omega turbulence model

Fluid Velocity	Erosion Rate Density (Kg/m^2s)	Maximum Induced Pressure (Pa)
3.8 m/s	5.94	5742
4.8 m/s	6.51	6682
5.8 m/s	8.44	9721

The erosion rate density is also significantly higher than the ones obtained from the standard k-ε model for all velocities. The pressure prediction by the RNG k-ε model is higher than that of the k epsilon turbulence model. This behavior reflects better handling of high turbulence zones by the RNG k-ε model especially for intense pressure fluctuation. Table 8 shows the values obtained from the Tabakoff erosion model using the k omega turbulence model.

Table 8. Tabakoff erosion model using k omega turbulence model

Fluid Velocity	Erosion Rate Density (Kg/m^2s)	Maximum Induced Pressure (Pa)
3.8 m/s	12.84	9110
4.8 m/s	22.95	10212
5.8 m/s	25.79	12015

The erosion rate density and maximum induced pressure for the Finnie and Tabakoff erosion models, as presented in Tables 6 and 7, are shown as functions of the fluid velocity using the k-ω turbulence model. As shown in Table 6, the Finnie model indicates that the erosion rate density increases from 5.94 kg/m^2s to 8.44 kg/m^2s at 3.8 m/s to 5.8 m/s while the maximum induced pressure increases from 5742 Pa to 9721 Pa thereby indicating a moderate erosion potential owing to lower impact force.

However, Table 7 shows that the Tabakoff model predicts very high erosion rates beginning at 12.84 kg/m^2s at 3.8 m/s and rising to 25.79 kg/m^2s at 5.8 m/s, with induced pressure increasing from 9110 Pa to 12015 Pa. This indicates the responsiveness of the Tabakoff model to velocity change and the ability to predict aggressive erosive mechanisms associated with high particle impact speeds, thus being appropriate for wear prediction in fast flow conditions. According to the k-ω turbulence model, we can see that the erosion rate density is higher than the one predicted by the k-ε and RNG k-ε models. This can be attributed to the fact that the k-ω model has the ability to model the near-wall turbulent fluctuation where most of the erosion takes place. A small increase in the erosion rate is observed with an increase in fluid velocity from 4.8 m/s to 5.8 m/s. Compared to the k-epsilon turbulence model, the k-ω model shows higher erosion rates mainly at 4.8 m/s and 5.8 m/s which signifies that the k-ω model is more sensitive to near-wall turbulence. The k-ω model is relatively better in simulating flow characteristics near walls of the pipe where erosion is predominant. The induced pressures also peak with the k-ω model, meaning evident turbulent pressure im-pulses near the wall are larger. The higher prediction of erosion rates and pressures by the k omega turbulence model can be attributed to the fact that the k-ω model is better capable of predicting boundary layer effects. High erosion rate zones are characterized by high shear and particle impacting velocities giving higher erosion rates and inducing pressure in turbulent flow.

3.4 Grid independence evaluation and validation

The highest erosion rate of 5.76 Kg/m^2s is observed at the tube where fluid enters, represented by the red-colored zones, which aligns closely with the results reported in the literature [27], thus confirming the accuracy of the findings. To ensure the reliability of the CFD simulations, a grid independence test was performed. The results, shown in Table 9, indicate that as the number of elements increased, the variations in both the velocity at the bend and the erosion rate density became negligible beyond 762,675 elements. This confirms that the grid resolution used in the final simulations is sufficiently refined to provide stable and accurate results.

Table 9. Grid independence test

Number of Elements	Velocity at Bend (m/s)	Erosion Rate Density (Kg/m^2s)
762,121	4.65	5.75
762,197	4.66	5.757
762,559	4.67	5.758
762,605	4.68	5.759
762,675	4.68	5.76

The number of mesh elements has slight variations, but the erosion rate density remains nearly the same and thus verifies the adequacy of the mesh configuration that was chosen.

4. DISCUSSION

The results from the CFD simulations show correspondingly clear trends in agreement with the theory. The Finnie erosion model has a more gradual, velocity-dependent wear mechanism than does the Tabakoff model, which is more comprehensive by accounting for the effects of particle velocity and impact angle and predicts lower erosion rates. The Tabakoff predicted higher erosion rates are in agreement with more intense particle impacts and turbulent flow conditions seen in the pipe bend. Both models find that the erosion rate is a constant density, increasing with increasing fluid velocity, which is expected as a result of the direct correspondence of particle velocity to impact energy. Nevertheless, the results of the Tabakoff model indicate an increasing rate of erosion with increasing velocity but show that it increases nonlinearly, meaning the magnitude of the rate increase in the critical velocity range can be approximately half of the rate at which it approaches the saturation region.

It may be that the high particle impact frequency at extremely high velocities is so high, that velocity increments have a progressively smaller effect on erosion rate growth. The

performance of the turbulence models explains the near-wall effects required for the prediction of erosion. This offers higher erosion rate and pressure pre-dictions with the k-ω model since it better encompasses the boundary layer phenome-non, specifically in regions where particle wall interaction governs, e.g. pipeline bends. On the other hand, the k-ε and RNG k-ε models have relatively good predictions, though they systematically underestimate near-wall turbulence, in particular in highly recirculating flows. Overall, the results were as expected. Velocity increases erosion rates, and increased turbulence increases particle wall interactions.

Comparisons of the models reveal that the choice of an erosion model and turbulence model is crucial and depends on the particular flow conditions and erosion mechanisms involved. Additionally, these insights generated from this study add a meaningful contribution to the understanding of erosion in particle-laden flows, particularly considering L-shaped pipelines. Trends observed are in line with prior research, thus validating the methodology. It is also worth noting the nonlinear increase in erosion rates predicted by the Tabakoff model at higher velocities, which presents a key consideration in pipeline design in high-stress environments.

Findings are also strengthened with comparisons to existing literature which consistently align with documented behaviors of erosion under similar circumstances. This also serves to illustrate the practical consequences of employing advanced models for turbulence such as k-ω that are more effective in capturing near-wall phenomena, relevant for industries faced with erosion-prone pipelines. The study bridges a critical gap in predictive modeling for slurry transport systems by systematically addressing both the gradual and high-impact erosion mechanisms.

5. CONCLUSIONS

From the CFD study conducted on an L-shaped pipeline, the effect of various operational parameters on erosion rate density is assessed. The numerical investigation conducted on the pipeline has shown that flow velocity has a significant effect on the location and magnitude of the erosion rate. Proper identification of high erosion rates is critical to identify susceptible zones of damage. The erosion rates and pressure results obtained from Finnie and Tabakoff models highlight the need to use appropriate pipeline materials and designs to deal with high-velocity fluids. The Tabakoff model indicates a higher potentiality of erosion due to the particle dynamic, and according to this model, both the fluid velocity and the size of the particle are the important factors directly affecting the pipeline's strength. The Finnie erosion model has provided a lower prediction of erosion rate density due to lesser consideration of particle impinging velocity. The Tabakoff erosion model has predicted erosion rates which are much higher than the Finnie model.

This can be attributed to the additional consideration of impact velocity by the Tabakoff model. The comparison of the Finnie and Tabakoff erosion models through different turbulence models (k-ε, RNG k-ε, and k-ω) have brought to light the strong correlation between the velocity of the fluid, turbulence, and erosion in pipeline systems that transport slurry. Erosion rate density as well as the maximum induced pressure increases for all models at higher levels of fluid velocity with varying levels of gradients. In comparison to the Finnie model the Tabakoff erosion model results in generally higher erosion rates especially at larger velocities. The turbulence models indicated the k-ω turbulence model to be the most accurate one as far as near-wall turbulence and boundary layer effects are concerned – and as such, it yields the greatest erosion rates and induced pressures. It is seen from the above figures that the RNG k-ε model exhibits slightly higher erosion rates than the standard k-ε model and both models underestimate the erosion rates and pressures as compared with the k-ω model. The research hypothesis that optimized pipeline design which accounts for fluid velocity and particle dynamics is able to substantially decrease erosion rates is shown to yield the result of validated findings. The findings indicate that the Finnie model is more suitable for low-velocity flows, where gradual erosion occurs due to shallow particle impact angles, while the Tabakoff model is more reliable for high-velocity flows, where severe material loss results from high-impact collisions. This distinction is critical for practical applications, as selecting the appropriate model based on flow conditions enhances the accuracy of erosion predictions, ultimately aiding in pipeline material selection and design optimization to mitigate long-term damage. The research questions directly guided the study that demonstrated that the geometric characteristics of elbows have a major impact on erosion most significantly in high-velocity zones. Moreover, it emphasized selecting suitable pipeline materials and protective coatings to level the effects of high-velocity fluid flow. It also showed that pipeline erosion can be reduced by both adjusting the fluid flow patterns and by changing the velocity and turbulence near the walls. Although the CFD results proved to be very beneficial, some limitations must betaken into consideration. Second, the models relied on assumptions that relatively limited particle distribution and that of ideal turbulence, which might not capture the actual pipeline conditions. Furthermore, the lack of experimental validation limits the amount ofcross-checking these numerical predictions to actual test data. Another limitation is the assumption of (spherical) particles, which may not fully reflect the irregular shape typical of slurry flows and affect the precision of the erosion predictions. Further research is needed to validate these CFD predictions through experimental testing to validate that the numerical models agree with actual conditions. In addition, the effectiveness of advanced materials and protective coatings in mitigating erosion in high-velocity flows will be further investigated. Studies for finding the best fluid flow pattern in critical regions could be expanded to reduce erosion, especially minimizing turbulence close to the pipe walls. Furthermore, the realism of future erosion models will increase by accounting for more complex particle dynamics, such as irregular shapes and different particle sizes. At last, the long-term performance of pipeline materials exposed to sustained, high-velocity, particle-laden flowing conditions is investigated to better understand the degradation and durability of materials over time.

REFERENCES

[1] Hussain, M., Zhang, T., Dwight, R., Jamil, I. (2024). Energy pipeline degradation condition assessment using predictive analytics–challenges, issues, and future directions. Journal of Pipeline Science and Engineering, 4(3): 100178. https://doi.org/10.1016/j.jpse.2024.100178

[2] Aryai, V., Baji, H., Mahmoodian, M. (2022). Failure

assessment of corrosion affected pipeline networks with limited failure data availability. Process Safety and Environmental Protection, 157: 306-319. https://doi.org/10.1016/j.psep.2021.11.024

[3] Xie, M., Zhao, J., Pei, X. (2023). Maintenance strategy optimization of pipeline system with multi-stage corrosion defects based on heuristically genetic algorithm. Process Safety and Environmental Protection, 170: 553-572. https://doi.org/10.1016/j.psep.2022.12.041

[4] Azzam, M. (2023). Failure analysis of pipelines in the oil and gas industry. In Pipeline Engineering—Design, Failure, and Management.

[5] Finnie, I. (1960). Erosion of surfaces by solid particles. Wear, 3(2): 87-103. https://doi.org/10.1016/0043-1648(60)90055-7

[6] Tabakoff, W., Kotwal, R., Hamed, A. (1979). Erosion study of different materials affected by coal ash particles. Wear, 52(1): 161-173. https://doi.org/10.1016/0043-1648(79)90206-0

[7] Zhang, J., Yi, H., Huang, Z., Du, J. (2019). Erosion mechanism and sensitivity parameter analysis of natural gas curved pipeline. Journal of Pressure Vessel Technology, 141(3): 034502. https://doi.org/10.1115/1.4043011

[8] Wang, Z.B., Zheng, Y.G. (2021). Critical flow velocity phenomenon in erosion-corrosion of pipelines: Determination methods, mechanisms and applications. Journal of Pipeline Science and Engineering, 1(1): 63-73. https://doi.org/10.1016/j.jpse.2021.01.005

[9] Liu, Y., Zhao, Y., Yao, J. (2021). Synergistic erosion–corrosion behavior of X80 pipeline steel at various impingement angles in two-phase flow impingement. Wear, 466: 203572. https://doi.org/10.1016/j.wear.2020.203572

[10] Chung, R.J., Jiang, J., Pang, C., Yu, B., Eadie, R., Li, D.Y. (2021). Erosion-corrosion behaviour of steels used in slurry pipelines. Wear, 477: 203771. https://doi.org/10.1016/j.wear.2021.203771

[11] Li, B., Li, W., Zeng, M., Wang, Q. (2021). Investigation on erosion of continuous bending pipes in different directions. Chemical Engineering Transactions, 88: 355-360. https://doi.org/10.3303/CET2188059

[12] Wang, S., Shi, J., Han, X., Zhu, L., et al. (2022). Effect of pipe orientation on erosion of π-shaped pipelines. Powder Technology, 408: 117769. https://doi.org/10.1016/j.powtec.2022.117769

[13] Othman, N.T.A., Putra, Z.A., Abidin, S.A.Z., Ali, F.I.M. (2023). CFD analysis of erosion rate in oil and gas pipeline industry. Jurnal Teknologi (Sciences & Engineering), 85(6): 59-66. https://doi.org/10.11113/jurnalteknologi.v85.20473

[14] Yu, H., Liu, H., Zhang, S., Zhang, J., Han, Z. (2023). Research progress on coping strategies for the fluid-solid erosion wear of pipelines. Powder Technology, 422: 118457. https://doi.org/10.1016/j.powtec.2023.118457

[15] Balasubramanian, V., Jain, M.C., Golovin, K., Zarifi, M.H. (2023). Real-time non-destructive erosion monitoring of coatings using passive microwave split ring resonator sensor. In 2023 IEEE International Conference on Consumer Electronics (ICCE), Las Vegas, NV, USA, pp. 1-4. https://doi.org/10.1109/ICCE56470.2023.10043427

[16] Xu, J., Lian, Z., Hu, J., Luo, M. (2018). Prediction of the maximum erosion rate of gas–solid two-phase flow pipelines. Energies, 11(10): 2773. https://doi.org/10.3390/en11102773

[17] Li, C., Bin, G., Li, J., Liu, Z. (2021). Study on the erosive wear of the gas-solid flow of compressor blade in an aero-turboshaft engine based on the Finnie model. Tribology International, 163: 107197. https://doi.org/10.1016/j.triboint.2021.107197

[18] Teran, L.A., Laín, S., Rodríguez, S.A. (2021). Synergy effect modelling of cavitation and hard particle erosion: Implementation and validation. Wear, 478: 203901. https://doi.org/10.1016/j.wear.2021.203901

[19] Wee, S.K., Yap, Y.J. (2019). CFD study of sand erosion in pipeline. Journal of Petroleum Science and Engineering, 176: 269-278. https://doi.org/10.1016/j.petrol.2019.01.001

[20] Rahimi-Larki, M., Vollmann, S., Jin, S. (2024). Flow-induced erosion modelling of cohesive material with coupled CFD-DEM approach. Minerals Engineering, 217: 108947. https://doi.org/10.1016/j.mineng.2024.108947

[21] Veiskarami, A., Saidi, M. (2024). Numerical analysis of gas-solid flow erosion in different geometries as alternatives to a standard pipe elbow. Powder Technology, 448: 120334. https://doi.org/10.1016/j.powtec.2024.120334

[22] Zhang, J., Li, H., Liu, H. (2024). Modeling of particle erosion of high-pressure turbine based on dynamic mesh method. Aerospace Science and Technology, 150: 109236. https://doi.org/10.1016/j.ast.2024.109236

[23] Okafor, E., Ibeneme, I.O. (2019). Parametric analysis of sand erosion in pipe bends using computational fluid dynamics. International Journal of Engineering Science, 3(6): 60-65.

[24] Zhang, Y., Jia, Y.F., Sun, X.W., Fang, Z.H., Yan, J.J., Zhang, C.C., Zhang, X.C. (2024). A model of erosion rate prediction for component with complex geometry based on numerical simulation. Wear, 546: 205328. https://doi.org/10.1016/j.wear.2024.205328

[25] Agarwal, A., Batista, R.C., Gurung, A. (2024). Analyzing the impact of bumper height on pedestrian injuries using explicit dynamics. In Smart Electric and Hybrid Vehicles, pp. 57-89.

[26] Agarwal, A., Dinka, M.O., Ilunga, M. (2024). Enhancing engine cylinder heat dissipation capacity through direct optimization (DO) techniques. Processes, 12(12): 2659. https://doi.org/10.3390/pr12122659

[27] Li, X., Fang, Y., Guo, Y., Li, X. (2023). Slurry discharge pipeline damage and wear due to transporting rock particles during slurry shield tunneling: A case study based on in situ observed results. Applied Sciences, 13(12): 7103. https://doi.org/10.3390/app13127103

[28] Agarwal, A., Kalenga, M.K.W., Ilunga, M. (2025). CFD simulation of fluid flow and combustion characteristics in aero-engine combustion chambers with single and double fuel inlets. Processes, 13(1): 124. https://doi.org/10.3390/pr13010124

[29] Agarwal, A., Ilunga, M., Tempa, K., Humagai, B. (2024). CFD analysis of solar air heater using V-shaped artificial roughness to attain heat transfer enhancement. International Journal of Energy Production and Management, 9(3): 171-180. https://doi.org/10.18280/ijepm.090306

[30] Yarasai, S.S., Ravi, D., Yoganand, S., Rajagopal, T.K.R.

(2023). Numerical investigation on the performance and combustion characteristics of a cavity based scramjet combustor with novel strut injectors. International Journal of Hydrogen Energy, 48(14): 5681-5695. https://doi.org/10.1016/j.ijhydene.2022.11.150
[31] Wang, H. (2023). A Guide to Fluid Mechanics. Cambridge University Press.
[32] Schalau, S., Habib, A., Michel, S. (2023). A modified k-ε turbulence model for heavy gas dispersion in built-up environment. Atmosphere, 14(1): 161. https://doi.org/10.3390/atmos14010161
[33] Lopez, A., Stickland, M., Dempster, W. (2015). Modeling erosion in a centrifugal pump in an Eulerian-Lagrangian frame using OpenFOAM®.Open Engineering, 5(1): 274-279. https://doi.org/10.1515/eng-2015-0037
[34] Khawaja, H., Moatamedi, M. (2018). Semi-implicit method for pressure-linked equations (SIMPLE)–solution in MATLAB®. The International Journal of Multiphysics, 12(4): 313-326.

NOMENCLATURE

ρ	the fluid density
u	the velocity vector
k	the turbulent kinetic energy
μt	the turbulent viscosity
σk	the turbulent Prandtl number for k
Gk	the generation of turbulence kinetic energy due to mean velocity gradients
ϵ	the dissipation rate of turbulent kinetic energy
dM/dt	the erosion rate as a function of time
N	impact rate of particles (number of impacts per unit time)
dM	the rate of mass loss of the material (erosion rate)
p	pressure
μ	dynamic viscosity
g	gravitational acceleration vector
F	additional forces (like particle interaction)
C	material dependent constant
$f(\theta)$	a function of the impact angle θ